Lasers in Medical Science (2022) 37:1333–1341
https://doi.org/10.1007/s10103-021-03399-7

ORIGINAL ARTICLE

Plasmonic hyperthermia or radiofrequency electric field hyperthermia of cancerous cells through green-synthesized curcumin-coated gold nanoparticles

Abbas Rezaeian[1] · Seyed Mohammad Amini[2] · Mohammad Reza H. Najafabadi[3] · Zohreh Jomeh Farsangi[4] · Hadi Samadian[5]

Received: 30 April 2021 / Accepted: 6 August 2021 / Published online: 18 August 2021

Abstract

Nanoparticle-mediated hyperthermia is one of the prominent adjuvant therapies which has been faced by many problematic challenges such as efficiency and safety. To compare the nanoparticle-mediated photothermal therapy and radiofrequency electric field hyperthermia, green-synthesized curcumin-coated gold nanoparticles (Cur@AuNPs) were applied in an in vitro study. Using recently published methodologies, each step of the study was performed. Through green chemistry, curcumin was applied as both a reducing and a capping agent in the gold nanoparticle synthesis process. Various techniques were applied for the characterization of the synthesized nanoparticles. The heating rate of Cur@AuNPs in the presence of RFEF or laser irradiation was recorded by using a non-contact thermometer. The cellular uptake of the Cur@AuNPs was studied by ICP-AES. The cellular viability and apoptosis rate of different treatment were measured to investigate the effect of two different nano-hyperthermia techniques on the murine colorectal cancer cell line. The average size of Cur@AuNPs was 7.2 ± 3.3 nm. The stability of the gold nanoparticles in the phosphate buffer saline with and without fetal bovine serum was verified by UV–Vis spectroscopy. FTIR, UV–Vis spectroscopy, and TEM indicate that the stability is a result of phenolic coating on the surface of nanoparticles. Cur@AuNPs can absorb both light and radiofrequency electric field exposure in a way that could kill cancerous cells in a significant number (30% in 64 µg/ml concentration). Green-synthesized Cur@AuNPs could induce apoptosis cell death in photothermal therapy and radiofrequency electric field hyperthermia.

Keywords Photothermal therapy · Radiofrequency electric field · Curcumin · Hyperthermia · Gold nanoparticles

✉ Seyed Mohammad Amini
Amini.sm@iums.ac.ir

Abbas Rezaeian
rezaiian.a@lums.ac.ir

Mohammad Reza H. Najafabadi
Hasani.njf@gmail.com

Zohreh Jomeh Farsangi
jomehfaz@mcmaster.ca

Hadi Samadian
h30samadiyan@gmail.com

[1] Department of Medical Physics, Lorestan University of Medical Sciences, Khorramabad, Iran

[2] Radiation Biology Research Center, Iran University of Medical Sciences (IUMS), 14003391769 Tehran, Iran

[3] Medical Nanotechnology Department, School of Advanced Technologies in Medicine, Tran University of Medical Sciences (IUMS), Tehran, Iran

[4] Department of Chemical Engineering, McMaster University, 1280 Main Street West, Hamilton, ON L8S 4L8, Canada

[5] Nano Drug Delivery Research Center, Health Technology Institute, Kermanshah University of Medical Sciences, Kermanshah, Iran

Introduction

Cancer hyperthermia has been considered an adjuvant for treatment such as chemotherapy or radiotherapy. A general definition of hyperthermia (thermal therapy or thermotherapy) is described as raising the temperature of cancerous tissues in a way that can sensitized cancerous tissue to the other modalities of treatments such as chemotherapy or radiotherapy. There is a huge amount of temperature chasm between hyperthermia and thermal ablation. Thermal ablation leads to the destruction of cancer tissue by severe hyperthermia. Generally, in thermal ablation therapy, the main cellular death mechanism is necrosis [1, 2].

Exposing the body to an external energy source to heat cancer cells in one area of the body requires a high intensity that can seriously damage healthy tissues through the necrotic process [3]. However, by loading the tumor cells with energy-adsorbent nanoparticles before the external energy exposure, a physician can avoid several of the barriers to achieve practical cancer hyperthermia. The gold nanoparticle is one of the most prominent nanoparticles with the capacity to adsorb various external energies in the hyperthermia process [4].

Photothermal therapy (PTT) which applied external laser irradiation was the most effective energy source for gold nanoparticle–mediated hyperthermia. However, recently, the energy-absorbing capability of the radiofrequency electric field (RFEF) has attracted many researchers for gold nanoparticle–mediated hyperthermia [5].

In this study, we have prepared and characterized Cur@AuNPs, investigated the cellular uptake and toxicity, and applied Cur@AuNPs in two different hyperthermia techniques. Curcumin acts as both a reducer and a stabilizer agent in the synthesis process, and no other chemicals were applied for the synthesis of gold nanoparticles. However, the main aim of this study was primarily to compare the gold nanoparticle–mediated photothermal therapy and gold nanoparticle–mediated radiofrequency electrical field hyperthermia (RFEF). Also, we could not apply every type of gold nanoparticle to both of the treatments. For RFEF hyperthermia, these particles must be smaller than 10 nm to interact with the RFEF. Also, the nanoparticles must be free of ionic background [5]. Furthermore, only two research groups have applied natural phenolic coated gold nanoparticles in PTT [6, 7]. As far as we know, no research group has applied these nanoparticles for RFEF hyperthermia. For the first time, we have studied the role of curcumin-coated gold nanoparticles in RFEF and PTT hyperthermia treatment.

Materials and methods

Chemical

Trachloroauric acid trihydrate 99.5% ($HAuCl_4$ $0.3H_2O$), curcumin, potassium carbonate (K_2CO_3), dimethyl sulfoxide (DMSO), hydrochloric acid (ACS reagent, 37%), and nitric acid (ACS reagent, 65%) were obtained from Merck chemicals company (Darmstadt, Germany) Ltd. RPMI-1640 culture medium (Biosera, UK) that is supplemented with 10% bovine serum albumin (Hyclone, UT, USA) and 1% penicillin/streptomycin (Hyclone, UT, USA) was applied for in vitro studies. Thiazolyl blue tetrazolium bromide (MTT) was purchased from Sigma-Aldrich (St. Louis, MO). Deionized water (resistivity of 18.3 MΩ.cm) that collected from Milli-Q Plus 185 water-purifying system (Millipore, Bedford, MA) was used for all aqueous solution. Glasswares were washed with Aqua Regia (a mixture of nitric acid and hydrochloric acid, 1:3) and rinsed thoroughly with DI water.

Synthesis and characterizations

With some modification, Cur@AuNPs were synthesized based on our previous study [8], 100 µl of a solution of cur in DMSO was added to the 15 ml of DI water in a round bottom flask. The pH of water has already been adjusted using K_2CO_3 (300 mM) before adding cur. After 3–5 min, 2.5 ml of $HAuCl_4.3H_2O$ (2.5 mM) was dropwise added to the solution, and the flask was left for 3 h under vigorous stirring. To complete the reaction, the Cur@AuNPs solution was aged for 3 days. Unreacted ions, DMSO, and cur molecules were eliminated through a series of centrifugation and decantation according to our previous study [6]. In the final round, the Cur@AuNPs were dispersed with a small volume of DI water to obtain higher concentrations of the nanoparticles. The gold concentration of the final product was assessed by ICP-AES analysis before further experiments. The size and morphology of the synthesized nanoparticles were studied by using a transmission electron microscope (Zeiss EM 900, Germany). UV–Vis spectroscopy analysis was performed by a double-beam UV–visible absorption spectrophotometer (SPEKOL 2000, Analytik Jena, UK) with 1 cm of optical path length quartz cuvette. The hydrodynamic diameter (DLS, NANO-flex Particle Sizer Germany) and Zeta potential (Zeta-check, Microtrac, Germany) analysis of Cur@AuNPs was performed by using the Nanoflex system. Fourier transform infrared (FTIR) spectra were collected from Nicolet Avatar 360 FTIR (Thermo Scientific, Courtaboeuf, France).

Temperature monitoring of Cur@AuNPs under RFEF or laser exposure

The heating rate of Cur@AuNPs in the presence of RFEF was studied by modified RFEF setup with the power of 100 Watt and at a frequency of 13.56 MHz (Basa Fan Company, Tehran, Iran). For photothermal heating studies, Cur@AuNPs with different concentrations were irradiated with a continuous-wave laser with a wavelength of 532 nm (Changchun New Industries Optoelectronics Technology Co., Ltd, Changchun, China). The sample temperatures under RFEF or laser exposure were read by a non-contact pyrometer system (THERMO-HUNTER SA-80 T-4 A, OPTEX, Shiga, Japan) mounted to a display and recording system. The specifications of setup with a schematic representation and pictures of each part are reported in our previous reports [5]. All the temperature readings have been adjusted for the offset temperature, and the heating responses were shown in a ΔT (°C). In all measures, the sample holder was a 1.5-ml microtube holding 1 ml of Cur@AuNPs or DIW as a control. Every test has been repeated, and the average of each test is represented as a heating graph of each concentration.

Cellular studies

Cellular analysis was conducted with mouse colorectal cancer (CT26) cell lines. Cells were incubated in a RPMI 1640 growth medium supplemented with fetal bovine serum (10%) and penicillin/streptomycin (1%) in a humified atmosphere (5% CO_2) at 37 °C. Cur@AuNP cellular uptake has been studied by the means of ICP-AES. Cells have been seeded in each well of 12 well-plates in a concentration of 300,000 cells per well. After 24 h, each well has been washed carefully three times, and then the cells have been separated by trypsin and transferred to the 5-ml volumetric balloon. The sample of each balloon has been digested by aqua regia, and gold content was analyzed by ICP-AES.

Cur@AuNP cytotoxicity investigation is conducted through the following procedure. A total of 10,000 cells were incubated into each well of 96-well plate (well bottom area = 0.32 cm^2), and after 24 h, the cell culture was substituted with fresh cell culture containing different concentrations of Cur@AuNPs and incubated for another 24 h. Before the MTT assay, cells were carefully washed with PBS. Thus, the free nanoparticles in the culture medium and the cell surface will be removed.

For plasmonic or radiofrequency electric field hyperthermia studies, after 24-h treatment of the cells with a specific concentration of Cur@AuNPs, the selected wells were washed gently with PBS and subsequently exposed with a continuous-wave laser (power density: 0.5 W/cm^2, 3 min) or radiofrequency electric field (13.5 MHz, 100 W, 3 min), and after that, the cell medium was substituted and the cells were incubated for another 24 h. On the next day, an MTT assay was carried out. In brief, cells have been incubated with 100 ml, 0.5 mg/ml solution of MTT in PBS for 2–4 h which was then replaced with 100 ml DMSO. The absorbance value of each well was read at a wavelength of 570 nm.

To analyze the percentage of apoptotic cells in different treatments and compare it with the control population, cells stained with annexin-5 (annexin V) and propidium iodide (PI) (eBioscience, San Diego, CA, USA) kite. CT26 cells have been seeded, incubated with Cur@AuNPs, and exposed to the RFEF or laser in three consecutive days. Next, cells were trypsinized, collected, and suspended in a 1 × buffer at a concentration of 10^6 cells/ml. Then, 5 ml of PI and 5 ml of annexin V–FITC were poured into the above 1 × binding buffer and the suspension was incubated in the dark for 20 min at room temperature. Finally, the interpretation of cell apoptosis was carried out by flow cytometry.

Statistical analysis

All data were shown as mean ± SD. For comparisons of the significance of the experimental data, the one-way analysis of variance (ANOVA) was applied. Statistical significance, α, was set to $p < 0.05$. The following software has been employed for analyzing or plotting of data: Origin 2015 (OriginLab Co., USA), GraphPad Prism 6 (GraphPad Software, San Diego, CA), digital micrographs, and Microsoft Excel.

Results and discussions

Synthesis and characterizations

Cur@AuNP synthesis and stability were confirmed by UV–Vis spectroscopy. The unreacted cur and ion removal was investigated by obtaining the UV–Vis spectra of the supernatant in every step of centrifugation and decantation. The fourth supernatant does not have any adsorption values which indicate the absence of gold ions or curcumin molecules (Fig. 1a). Based on this test, all the samples were washed at least 5 times. The UV–Vis spectrum of the pristine Cur@AuNPs is similar to the 5 times washed sample. For biomedical application, the stability of gold nanoparticles in the physiological medium is very important. The stability of the Cur@AuNPs in PBS alone or PBS supplemented with FBS was also studied by UV–Vis spectra. If the nanoparticles are not stable in the presence of serum proteins or electrolyte solutions, they will not be applicable for cellular studies. After 64 days, no changes have been observed in the spectrum of PBS solution of Cur@AuNPs (Fig. 1b). By adding FBS to the PBS solution, the plasmonic shift of the particles was not shifted or broadened (Fig. 1c). Our

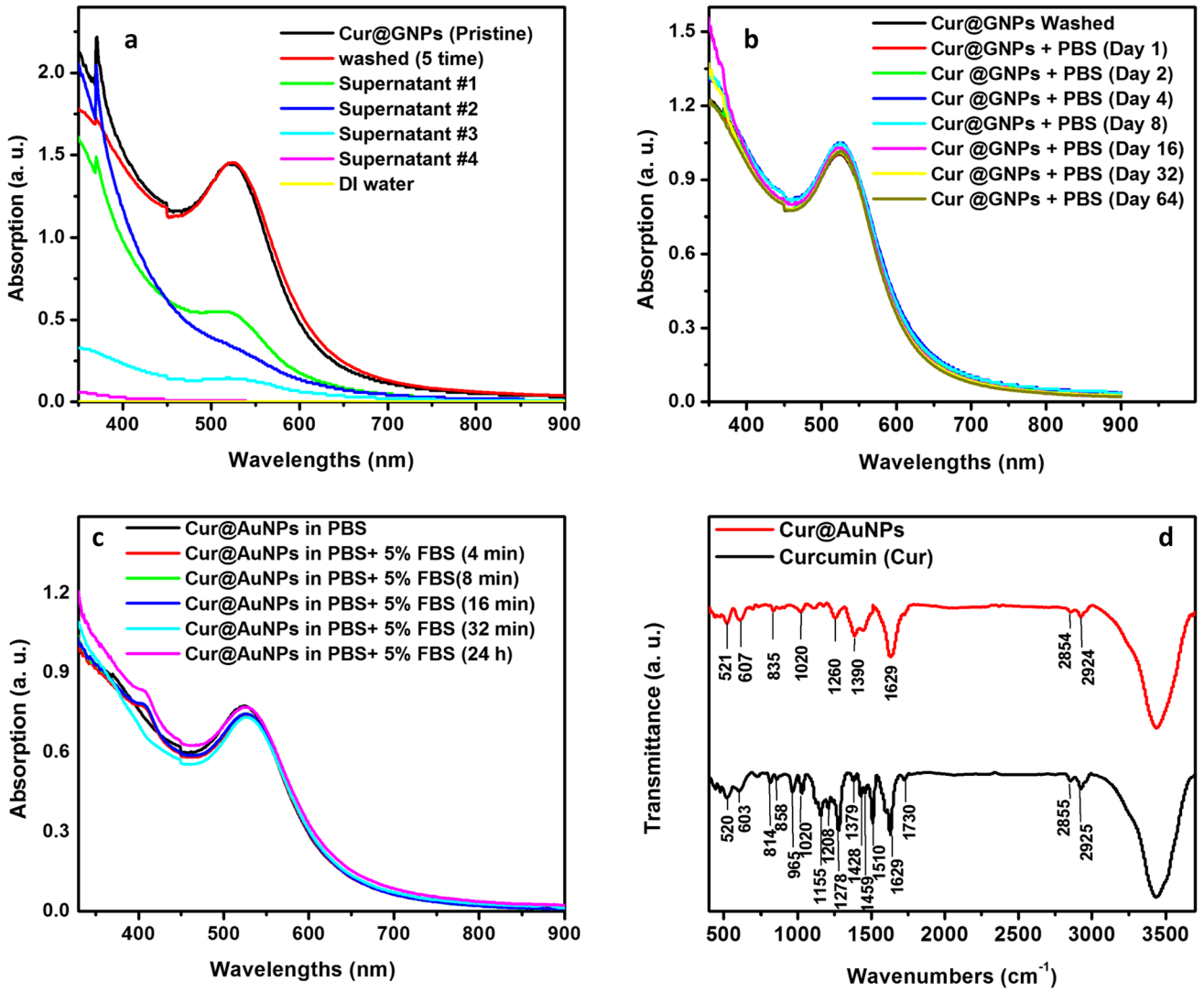

Fig. 1 Spectroscopic analysis of Cur@AuNPs. The UV–Vis spectra of pristine and five times washed Cur@AuNPs and supernatant of each washing step (**a**). The stability of washed Cur@AuNPs in 4 weeks in PBS medium (**b**) and in the presence of PBS + 5% FBS for 24 h (**c**). FTIR spectra of AuNPs, cur, and Cur@AuNPs (**d**)

hypothesis for the very good stability of Cur@AuNPs is the thick organic coating around the surface of the gold nanoparticles. FTIR spectroscopy was performed for the analysis of curcumin adsorption on the surface of gold nanoparticles (Fig. 1d).

Generally, both FTIR spectra are similar, and many peaks of cur spectrum were also repeated in the Cur@AuNP spectrum. In brief, a broad peak around 3400 cm^{-1} for cur and Cur@AuNPs is assigned for hydrogen bonding of ν O–H or phenol groups. A dual-band around 2920 and 2850 cm^{-1} was attributed to ν C-H stretching [9]. A stretching of C = C or vibrational (C = O) band observed in both samples occured at 1630 cm^{-1} [10]. Also, the presence of a specific curcumin band with a vibration stretching of C-O-C at 1020 cm^{-1} of both spectra is a direct indication of cur attachment on the surface of gold nanoparticles which has been reported before by Palmal et al. [11].

Some bands that represent the ring stretch in the cur spectrum (1428, 1459, 1510 cm^{-1}) [12] was absent in the Cur@AuNP spectrum. Also, the C = O stretching of the carbonyl functional group (1730 cm^{-1}) is observed for the cur spectrum only (Fig. 1d). The absence of carbonyl and ring stretch in Cur@AuNPs may be an indication of cur chemical binding on the surface of gold nanoparticles through these functional groups.

Also, the organic coating on the surface of gold nanoparticles on the TEM micrographs is visible (red arrows in Fig. 2). Phenolic coating in TEM micrographs of metal nanoparticles was observed before [13, 14]. The size, size distribution, and morphology of Cur@AuNPs were studied

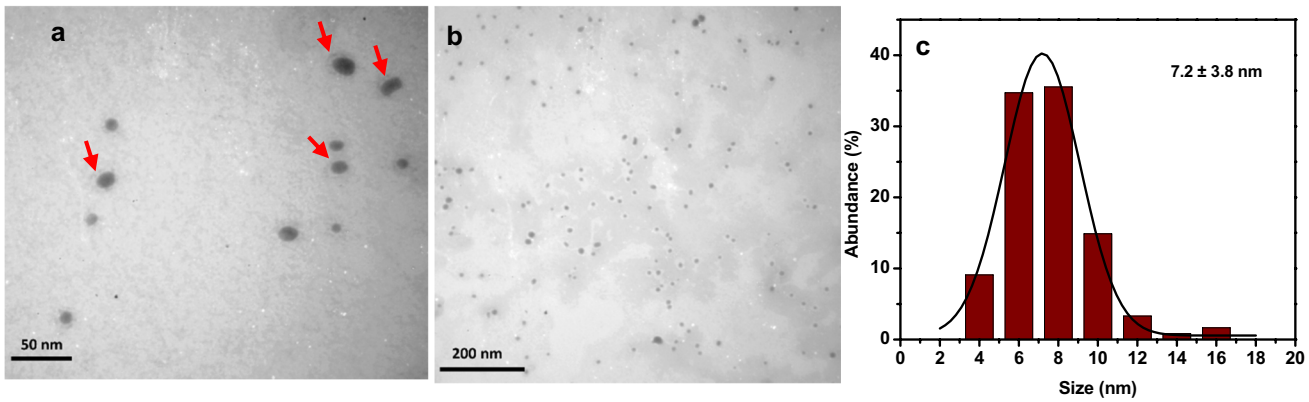

Fig. 2 TEM micrographs (**a**, **b**) and size distribution diagram (**c**) of Cur@AuNPs

by obtained TEM micrographs. The average diameter of the Cur@AuNPs was 7.2 ± 3.8 nm (Fig. 2a). Cur@AuNPs were round in shape and monodispersed in size (Fig. 2a, b).

Heating rate of Cur@AuNPs under RFEF or laser exposure

The scientific basis of plasmonic photothermal conversion is well-understood among researchers and is dependent on the plasmonic properties of the AuNPs [15, 16]. Rahimi-Moghaddam et al. have applied the curcumin-attached polyethylene glycol (PEG-Cur) for gold nanoparticle synthesis with an average diameter of 15.6 ± 3.2 nm. The synthesized nanoparticles represent an approximate plasmonic peak at 530 nm [7]. The laser wavelength for nanoparticle photothermal therapy must be selected based on the plasmonic peak of the gold nanoparticles. However, the PEG-Cur@AuNP-mediated photothermal destruction of cancerous cells was performed with a 808-nm diode laser [7]. Therefore, very high concentrations of PEG-Cur@AuNPs (2260, 22,600 µg/ml) and high laser power have been used to generate significant heat under 808-nm laser irradiation.

In our experiment, the heating rate of Cur@AuNPs was investigated under 532-nm laser irradiation which is similar to the plasmonic peak of the Cur@AuNPs. It has been observed that the heating rate of Cur@AuNPs depends on the nanoparticle concentration (Fig. 3a) which was predictable based on previous studies [15–18]. However, 7 nm is a very small size and it has been reported that by increasing the nanoparticle's size or volume, the photothermal conversion efficacy will be decreased [17]. The smaller the particle, the lower the absorption/scattering ratio, and most of the light energy in the smaller particles have been converted to heat energy [15, 18], but the total extinction has been reduced, which could limit the light adsorption [18]. Since the surface plasmonic resonance is the mechanism of gold nanoparticle heating under laser irradiation, increasing the concentration of gold nanoparticles, higher amount of lights will be adsorbed in the cancerous cells [19, 20].

We investigate the RFEF heating behavior of Cur@AuNPs. RFEF absorption capability of Cur@AuNPs was investigated by exposing the nanoparticles to the RFEF at room temperature based on our previous report [21]. At high concentrations (400 and 800 µg/ml), by applying RFEF, the heating rate of the Cur@AuNPs was very

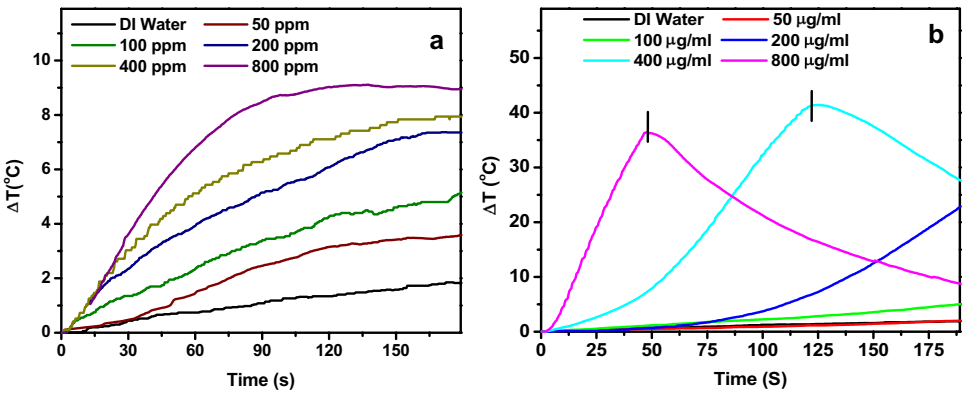

Fig. 3 Thermal response of Cur@AuNPs under laser (532 nm, 0.5 W/cm^2, 3 min) or RFEF exposure (13.5 MHz, 100 W). Thermal responses of Cur@AuNPs in different concentrations under laser irradiation (**a**), thermal responses of Cur@AuNPs in different concentrations under RFEF exposure (**b**)

high in a way that as the temperature of the nanoparticles solutions reaches 70 °C, the RFEF source is switched off which has been pointed by a short black line in the diagram (if applied). However, the lowest chosen concentration (50 µg/ml) under RFEF exposure, the temperature of Cur@AuNPs was not varied to a considering degree (Fig. 3b).

RFEF heating of gold nanoparticles is under huge scrutiny. There are many suggested mechanisms for RFEF heating of only sub 10-nm gold particles [4]. Joule heating of ionic backgrounds which came from the surface coating of the gold nanoparticles has been considered the source of heating at first [5]. Sassaroli et al. proposed the electrophoretic movement of the sub 10-nm gold nanoparticles [17]. And finally, it has been shown that very small gold clusters are paramagnetic and could heat under radiofrequency field [21, 22]. Since the Cur@AuNPs have an average diameter of 7 nm, all three mechanisms may play a role in the observed heating (Fig. 3b). However, unreacted Au ion or curcumin has been removed from Cur@AuNPs through a series of centrifugation and decantation. So joule heating was not from free ions or charged molecules in the solution. However, there is a phenolic coating on the gold nanoparticles that could be the source of the Joule heating.

Cellular studies

The safety and toxicity of nanoparticles are the main pillar of its biomedical application. The metal nanoparticles that have been synthesized by plant-derived compound are being considered safe by many researchers [14]. However, we applied MTT assay for testing the cytotoxicity of Cur@AuNPs. Our MTT assay revealed that the gold nanoparticles were not toxic even up to 128 µg/ml concentration (Fig. 4a). No cytotoxicity or very low cytotoxic effect was reported for curcumin-coated gold nanoparticles in various cells such as murine fibroblast [8], peripheral blood lymphocytes [23], marrow-derived macrophages [24], and human prostate cancer cells [25]. However, each research group applied slightly different particles, but it has been considered that curcumin-coated gold nanoparticles are very biocompatible.

Low cytotoxicity of Cur@AuNPs raises a question about cellular uptake of the particles. Cellular uptake of the gold nanoparticles on CT26 has been carried out at three different concentrations. Concentration-dependent cellular uptake of gold nanoparticles has also been observed for citrate- [26] and folate [27]-coated gold nanoparticles. By increasing the concentration of gold nanoparticle, the uptake value was increased in CT26 cell lines. In addition to the concentration and surface chemistry, the cellular uptake of the gold nanoparticles also depends on particle size [28], surface charge,

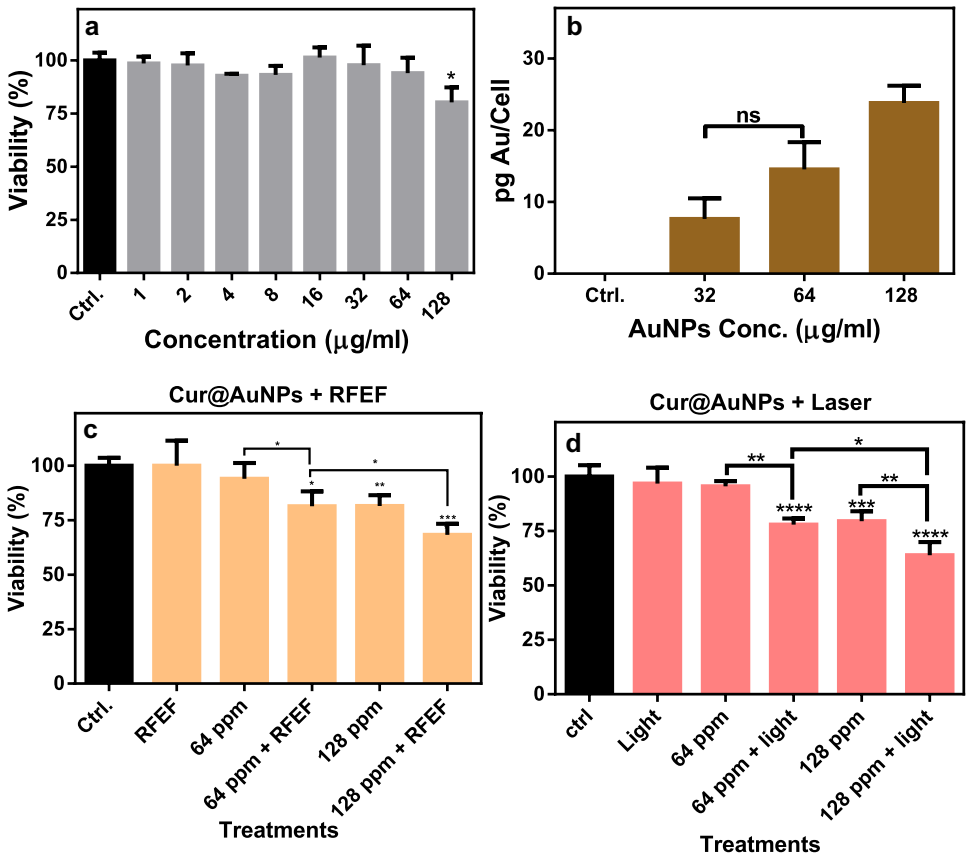

Fig. 4 Cellular analysis: cell viability of Cur@AuNPs after 24-h treatment with Cur@AuNPs through MTT assay (**a**). CT26 cellular uptake of Cur@AuNPs investigation through ICP-AES (**b**). The viability of CT26 cancerous cells after 24-h treatment with Cur@AuNPs and 3-min exposure of RFEF(13.5 MHz, 100 W), (**a**) or 3-min laser irradiation (power density: 0.5 W/cm^2) (**b**)

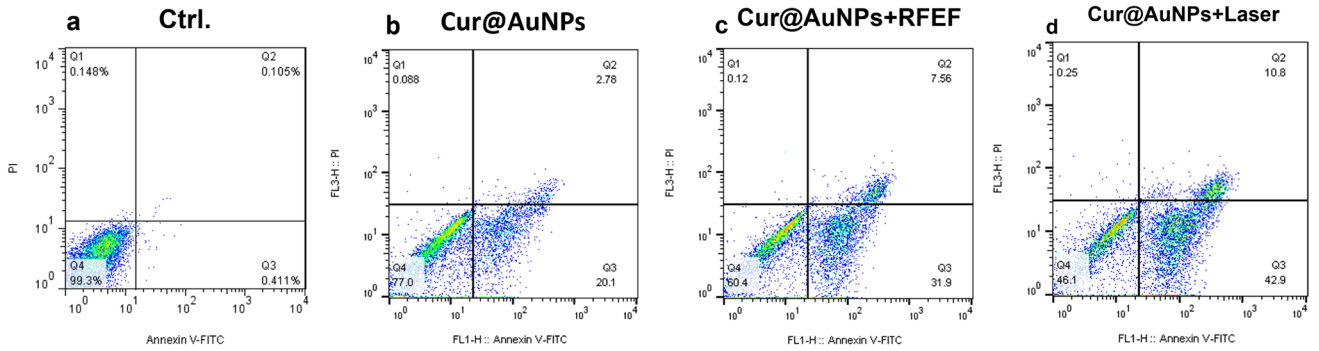

Fig. 5 Assessment of cell death mechanism by annexin V-PI staining in CT26 cells after the treatment of cells with 128 µg/ml Cur@AuNPs (**b**), 128 µg/ml Cur@AuNPs plus RFEF (13.5 MHz, 3 min) (**c**), and 128 µg/ml Cur@AuNPs plus laser (0.5 W/cm^2, 3 min) (**d**). Ctrl. represents the control population (**a**)

and the shape of the particles [29]. The low percentage of cellular adsorption of Cur@AuNPs (Fig. 4b) can be due to their negative charge (-22.2 ± 1.5 mV). Also, it has been shown that the protein serum could interact with Cur@AuNPs and reduce the cellular uptake of Cur@AuNPs [25].

Photothermal and electric field treatment of colorectal cancerous cells has been performed in both of the concentrations that have been studied in cellular uptake analysis. Both RFEF and laser treatment could increase cell death in a significant value; however, in either of the treatment, most of the cancerous cells remain alive. In both concentrations of Cur@AuNPs, the amount of cellular death in cells that have been exposed to the laser is significantly higher in comparison with those that have been exposed to the RFEF (Fig. 4c, d).

Based on the cellular analysis, the Cur@AuNPs could increase the photothermal destruction of cells under laser irradiation. The observed photothermal effect is demonstrated to be dependent to concentration (Fig. 4d). However, increasing the concentration of Cur@AuNPs from 64 to 128 µg/ml did not significantly increase cell death under RFEF treatment (Fig. 4c). Therefore, it can be concluded that in photothermal treatment, both laser irradiation and nanoparticle concentration play a crucial role in cell mortality. However, the concentration cannot play a decisive role in cell mortality under RFEF treatment, similar to laser treatment.

The death of the cells that have been pretreated with AuNPs under RFEF exposure is reported by many research groups; however, it is very hard to say that cell death is a direct result of hyperthermia [30]. It has been shown that the RFEF treatment could change the cellular phenotypes of cancer cells including the mechanical integrity of the cells. Alterations of cells mechanical properties may change the nanoparticle uptake pathways [31]. Therefore, a small increase in cell death might be due to increased nanoparticles entering the cell rather than the direct result of Cur@AuNP-mediated RFEF hyperthermia. Also, the mitochondrial malfunction of cancerous cells that have been exposed by RFEF was observed [32]. However, it has been shown that sub 10 nanoparticles could be heated under RFEF, and the polarized coating such as cur might increase gold nanoparticle RFEF adsorption capacity [5, 21, 30].

To assess the degree of apoptotic percentage of cells that have been treated by each of the hyperthermia techniques, flow cytometry analysis was conducted. The diagrams in Fig. 5 depict the bivariate Annexin V/PI analysis of Cur@AuNPs alone and in combination with two hyperthermia treatment. The viable cells have a negative value for both compounds and are observed in the Q4 part of the diagram, while necrotic cells are PI-positive (Q1, Q2) and apoptotic cells are annexin V-positive (Q2, Q3).

Apoptosis is the natural way for a cell to die. Escaping apoptosis is the cancerous cell achievement that gives them the ability of continuous dividing. Utilizing the cell's mechanism for destruction is the best way for cancer treatment. Flow cytometry analyses revealed that the main cell death pathway of Cur@AuNP treatment alone or in combination with either of hyperthermia treatments is the apoptosis. However, similar to the MTT test, the rate of cell death is higher in PTT. Previous studies show that the Cur@AuNPs could induce apoptosis in cancerous cells [30, 31]. Other green-synthesized gold nanoparticles through plant phenolic compounds such as apigenin [32] and kaempferol [33] could also induce apoptotic cell death.

Conclusion

Gold nanoparticles are synthesized using natural curcumin antioxidant using a very simple method. The average size of these nanoparticles is 7.2 ± 3.8 nm. These nanoparticles are highly homogeneous and stable for at least 2 months

in physiological solutions such as phosphate buffer. Curcumin coatings exist on the surface of nanoparticles and have been demonstrated by spectroscopic and microscopic methods. The nanoparticles are highly biocompatible and do not cause a higher amount of cell death in the MTT test up to concentrations above 128 μg/ml. The use of lasers or electric fields can increase the mortality of cells that have been treated with Cur@AuNPs. The premier mechanism of cell death in both methods is apoptosis which indicates successful hyperthermia due to Cur@AuNPs. The cell death rate in photothermal therapy treatment is statistically dependent on Cur@AuNPs concentration. However, doubling the concentration of nanoparticles did not have a statistically significant effect on cell mortality in the RFEF hyperthermia experiment. Based on the results, we concluded that the gold nanoparticle–mediated PTT is more effective than gold nanoparticle–mediated RFEF hyperthermia.

Funding The current research has been supported by the Iran University of Medical Sciences (IUMS) under grant number 99–3-68–18954.

Data availability All authors make sure that all data comply with field standards.

Code availability Not applicable.

Declarations

Conflict of interest The authors declare no competing interests.

References

1. Van der Zee J (2002) Heating the patient: a promising approach? Ann Oncol 13(8):1173–1184
2. Wust P et al (2002) Hyperthermia in combined treatment of cancer. Lancet Oncol 3(8):487–497
3. Hildebrandt B et al (2002) The cellular and molecular basis of hyperthermia. Crit Rev Oncol Hematol 43(1):33–56
4. Amini SM (2019) Gold nanostructures absorption capacities of various energy forms for thermal therapy applications. J Therm Biol 79:81–84
5. Amini SM et al (2018) Radiofrequency electric field hyperthermia with gold nanostructures: role of particle shape and surface chemistry. Artif Cells Nanomed Biotechnol 46(7):1452–1462
6. Amini SM et al (2021) Investigating the in vitro photothermal effect of green synthesized apigenin-coated gold nanoparticle on colorectal carcinoma. IET Nanobiotechnol 15(3):329–337
7. Rahimi-Moghaddam F, Azarpira N, Sattarahmady N (2018) Evaluation of a nanocomposite of PEG-curcumin-gold nanoparticles as a near-infrared photothermal agent: an in vitro and animal model investigation. Lasers Med Sci 33(8):1769–1779
8. Shaabani E et al (2017) Curcumin coated gold nanoparticles: synthesis, characterization, cytotoxicity, antioxidant activity and its comparison with citrate coated gold nanoparticles. Nanomed J 4(2):115–125
9. Neshastehriz A et al (2020) In-vitro investigation of green synthesized gold nanoparticle's role in combined photodynamic and radiation therapy of cancerous cells. Adv Nat Sci Nanosci Nanotechnol 11(4):045006
10. Bich VT et al (2009) Structural and spectral properties of curcumin and metal-curcumin complex derived from turmeric (Curcuma longa). Physics and engineering of new materials. Springer, pp 271–278
11. Palmal S et al (2014) Inhibition of amyloid fibril growth and dissolution of amyloid fibrils by curcumin–gold nanoparticles. Chem A Eur J 20(20):6184–6191
12. Chidambaram M, Krishnasamy K (2014) Drug-drug/drug-excipient compatibility studies on curcumin using non-thermal methods. Adv Pharm Bull 4(3):309
13. Singh DK et al (2013) In situ synthesis and surface functionalization of gold nanoparticles with curcumin and their antioxidant properties: an experimental and density functional theory investigation. Nanoscale 5(5):1882–1893
14. Amini SM, Akbari A (2019) Metal nanoparticles synthesis through natural phenolic acids. IET Nanobiotechnol 13(8):771–777
15. Richardson HH et al (2009) Experimental and theoretical studies of light-to-heat conversion and collective heating effects in metal nanoparticle solutions. Nano Lett 9(3):1139–1146
16. Abadeer NS, Murphy CJ (2016) Recent progress in cancer thermal therapy using gold nanoparticles. J Phys Chem C 120(9):4691–4716
17. Sassaroli E, Li K, O'Neill B (2012) Radio frequency absorption in gold nanoparticle suspensions: a phenomenological study. J Phys D Appl Phys 45(7):075303
18. Mackey MA et al (2014) The most effective gold nanorod size for plasmonic photothermal therapy: theory and in vitro experiments. J Phys Chem B 118(5):1319–1326
19. Huang X et al (2007) The potential use of the enhanced nonlinear properties of gold nanospheres in photothermal cancer therapy. Lasers Surg Med 39(9):747–753
20. Karan NS et al (2015) Plasmonic giant quantum dots: hybrid nanostructures for truly simultaneous optical imaging, photothermal effect and thermometry. Chem Sci 6(4):2224–2236
21. Amini SM, Kharrazi S, Jaafari MR (2017) Radio frequency hyperthermia of cancerous cells with gold nanoclusters: an in vitro investigation. Gold Bulletin 50(1):43–50
22. Window PS, Ackerson CJ (2020) Superatom paramagnetism in Au102 (SR) 441–/0/1+/2+ oxidation states. Inorg Chem 59(6):3509–3512
23. Sindhu K et al (2011) Investigations on the interaction of gold–curcumin nanoparticles with human peripheral blood lymphocytes. J Biomed Nanotechnol 7(1):56–56
24. Heo DN et al (2014) Inhibition of osteoclast differentiation by gold nanoparticles functionalized with cyclodextrin curcumin complexes. ACS Nano 8(12):12049–12062
25. Nambiar S et al (2018) Synthesis of curcumin-functionalized gold nanoparticles and cytotoxicity studies in human prostate cancer cell line. Appl Nanosci 8(3):347–357
26. Movahedi MM et al (2018) Investigating the photo-thermo-radiosensitization effects of folate-conjugated gold nanorods on KB nasopharyngeal carcinoma cells. Photodiagn Photodyn Ther 24:324–331
27. Li G et al (2009) One-step synthesis of folic acid protected gold nanoparticles and their receptor-mediated intracellular uptake. Chem A Eur J 15(38):9868–9873
28. Coradeghini R et al (2013) Size-dependent toxicity and cell interaction mechanisms of gold nanoparticles on mouse fibroblasts. Toxicol Lett 217(3):205–216
29. Malugin A, Ghandehari H (2010) Cellular uptake and toxicity of gold nanoparticles in prostate cancer cells: a comparative study of rods and spheres. J Appl Toxicol 30(3):212–217

30. Sindhu K et al (2014) Curcumin conjugated gold nanoparticle synthesis and its biocompatibility. RSC Adv 4(4):1808–1818
31. Liu R et al (2019) Apoptotic effect of green synthesized gold nanoparticles from Curcuma wenyujin extract against human renal cell carcinoma A498 cells. Int J Nanomed 14:4091
32. Rajendran I et al (2015) Apigenin mediated gold nanoparticle synthesis and their anti-cancer effect on human epidermoid carcinoma (A431) cells. RSC Adv 5(63):51055–51066
33. Govindaraju S et al (2019) Kaempferol conjugated gold nanoclusters enabled efficient for anticancer therapeutics to A549 lung cancer cells. Int J Nanomed 14:5147–5157. https://doi.org/10.2147/IJN.S209773